Negative correlation between concentration of iron oxides and particulate matter in atmospheric dust: case study at industrial site during smoggy period

Eduard Petrovský[1], Aleš Kapička[1], Hana Grison[1], Bohumil Kotlík[2], Hana Miturová[3]

1 Institute of Geophysics, Czech Academy of Sciences, Boční II/1401, 14100 Prague 4, Czech Republic

2 National Institute of Public Health, Šrobárova 48, 100 42 Prague 10, Czech Republic

3 Public Health Institute Ostrava, Partyzánské nám. 7, 702 00 Ostrava, Czech Republic

Corresponding author: E. Petrovský (edp@ig.cas.cz)

Abstract

Background: Environmental magnetism, focusing on ferrimagnetic iron oxides, provides useful additional information on pollution of different environments. Magnetic methods have been applied to studies of atmospheric dust, namely PM10 (particulate matter smaller than 10 micrometers) in, e.g., industrial or urban areas. Until now, positive correlation was reported between concentration of iron oxides (expressed in terms of either magnetic susceptibility, saturation remanent or saturation induced magnetization) and concentration of PM10 or smaller. Purpose of this study was to verify the relationship between iron oxides and PM at monitoring site close to source of emissions rich in iron oxides during period of smoggy conditions.

Results: We examined 24-hours PM10 and PM1 samples, collected during 10 days of smoggy winter period at a site close to steel plant, which represents a significant source of atmospheric emissions in industrial region of Northern Moravia (Czech Republic), known for generally high degree of air pollution. Magnetic hysteresis loops were measured in order to obtain parameters reflecting the concentration and grain-size distribution of iron oxides. Our data show unexpected negative correlation between saturation magnetization (concentration of ferrimagnetic iron oxides) and both PM1 and PM10 concentrations, to the best of our knowledge the trend not being reported yet.

Conclusions: Our finding may seemingly disqualify magnetic methods as useful proxy in air pollution studies. However, we suggest that this is an exceptional case, specific to this region and monitoring site, as well as to synoptic conditions during the smoggy period. Although the significant dust

emissions are presumably rich in iron oxides, the overall air quality at the monitoring site is determined by the general environment, controlled by many other sources of different character in the region, and by the specific climatic conditions. Thus, the nearby steel plant, presumably emitting dust rich in ferrimagnetic iron oxides, dominates the deposited dust at the nearby monitoring site only during very few days of suitable weather (namely wind speed and direction).

Keywords: environmental magnetism, magnetite, atmospheric dust, pollution, steel works, correlation

Background

Environmental magnetism applies rock-magnetic methods to assess the composition, concentration, and grain-size distribution of ferrimagnetic iron oxides, namely magnetite and maghemite. Originally developed for the study of historical records of geomagnetic field and its changes in rocks (paleomagnetism), these methods are now also used to study magnetic properties of, e.g., sediments, soils, atmospheric dust and its biocarriers (tree leaves and needles, lichens, mosses), mainly in order to establish the correlation between magnetite (and/or maghemite) and environmentally-significant parameters, such as concentration of heavy metals or particulate matter of specific size (PM10), and thus to assess the environmental stress reflected by the presence of these minerals. Muxworthy et al. (2001) investigated samples of respirable atmospheric particulate matter collected in Munich, Germany, and compared them with pollution and meteorological data. The primary magnetic mineral identified was magnetite in the grain-size range 0.2-5 μm and concentrations of 0.3-0.6% in mass. Saturation remanent magnetization (Mrs) of daily samples of PM10, collected at two sites in Munich, Germany, was found to be strongly correlated with the PM mass, with the magnetite concentration being 0.3-0.5% by mass (Muxworthy et al., 2003). Magnetite as the dominant magnetic mineral was identified in particulate matter 10 μm or less in diameter (PM10) collected at sites with different level of air pollution also by Petrovsky et al. (2013). Sagnotti et al. (2006) reported on the magnetic properties of PM10 samples collected by six automatic stations installed for air quality monitoring through the Latium Region (Italy). In addition to magnetic

parameters reflecting the composition, concentration and grain size distribution of iron oxides, Sagnotti et al. (2006) examined also low-field magnetic susceptibility and found high positive correlation with PM10. More details on composition, concentration and grain size distribution of magnetic fraction deposited on tree leaves as well as collected by automated monitoring station in Rome were published by Sagnotti et al. (2009). Magnetic properties of tree leaves as biocarriers of the deposited atmospheric dust have been investigated in relation to air pollution by many authors (Hofman et al., 2017; Jordanova et al., 2010b; Jordanova et al., 2003; Kardel et al., 2018; Kardel et al., 2011; Kardel et al., 2012; Maher et al., 2008; Matzka and Maher, 1999; Mitchell and Maher, 2009; Mitchell et al., 2010; Moreno et al., 2003; Rodriguez-Germade et al., 2014; Sagnotti et al., 2009; Zhang et al., 2006). There are also numerous studies on magnetic properties of tree needles (Jordanova et al., 2010; Lehndorff et al., 2006; Urbat et al., 2004), tree barks, rings or branches (Brignole et al., 2018; Vezzola et al., 2017; Wuyts et al., 2018; Zhang et al., 2009; Zhang et al., 2008), lichens, in situ or transplanted (Chaparro et al., 2013; Kodnik et al., 2017; Marie et al., 2016; Marie et al., 2018; Paoli et al., 2017; Salo et al., 2012), and moss and transplanted moss bags (Fabian et al., 2011; Limo et al., 2018; Salo et al., 2012, 2016a, 2016b; Salo and Makinen, 2014, 2019; Vukovic et al., 2015a; Vukovic et al., 2015b). High sensitivity of magnetic methods enabled even examination of magnetic properties of spider webs (Rachwal et al., 2018). Magnetic measurements of different carriers of atmospherically deposited dust particles have unambiguously several advantages: very high sensitivity in terms of concentration of ferrimagnetic iron oxides, non-destructive character, ability to investigate short-term (daily samples) as well as long-term deposition (months to years), and/or possibility to be applied in remote places without any infrastructure and electricity (transplanted lichens and moss bags). However, it has to be emphasized that the results in terms of air pollution are site specific; correlation with environmentally important parameters has to be established for each study site independently. It seems also clear that saturation magnetization (either remanent or induced) is more sensitive and reliable magnetic parameter compared to

magnetic susceptibility, the use of the latter one as a rapid method of assessing the bulk magnetic content of atmospheric particulate matter could be misleading.

Finally, to the best of our knowledge, all the studies reported on positive correlation between concentration of ferrimagnetic iron oxides and particulate matter, either PM10 or smaller. In this study, we examine daily PM10 and PM1 samples collected by automatic high-volume samplers at industrial monitoring site located very close to the iron smelter during smoggy period, characterized by very high level of air pollution. Magnetite was determined as the main magnetic fraction in PM10 collected at the same monitoring station in our previous study (Petrovsky et al., 2013). The aim of the present study was to determine the relationship between concentration of magnetite and PM at this specific industrial site, where we assumed that magnetite is predominantly of industrial origin, emitted from the steel plant. Moreover, due to the specific climatic conditions during the smoggy period the emitted dust is supposed to remain in the close neighbourhood of the source.

Samples and Methods

Daily samples of PM10 and PM1 (20 samples each) were collected from 30 January to 7 February 2012 using two parallel Grasseby-Andersen high-volume samplers during day and night time (thus representing 12 hours accumulation) on acetyl-nitrocellulose filters at monitoring station “Ostrava Radvanice ZU” (formerly Ostrava Bartovice, GPS 49°48'25.4"N 18°20'20.9"E, altitude of 263 m a.s.l., Fig. 1). This period was characterized by smoggy conditions, with PM10 daily average concentrations well above 50 $\mu g/m^3$ (Table 1). After this period, when the daily PM10 values dropped below the limit of 50 $\mu g/m^3$, additional sampling from 16 to 18 February was carried out in order to obtain samples for comparison.

The station belongs to automatic monitoring network of the Czech Hydrometeorological Institute (www.chmi.cz). It is located in residential area, about 50 m from major road and some few hundreds of meters from major steel works to the south-west (Fig. 1). According to the EOI 97/101/EC document (https://eur-lex.europa.eu/legal-

content/EN/TXT/PDF/?uri=CELEX:31997D0101&from=EN), the station is classified as industrial, and the zone is characterized as industrial/suburban/residential (http://portal.chmi.cz/files/portal/docs/uoco/web_generator/locality/pollution_locality/loc_TORE_GB.html). The spatial representativeness of the station is within the microscale of 100 m. The site is considered as one with the most polluted atmosphere in the Czech Republic. In 2012, the maximum of daily average concentration of PM10, was 281.3 μg/m^3, median was 35.2 μg/m^3, the daily limit of PM10 was exceeded during 166 days. The annual average concentration of PM10 was 49.5 μg/m^3 (data based on automatic monitoring using the optoelectronic method, CHMI, 2012). Data for PM1 are not available for that period, only PM10 and PM2.5 were monitored automatically. The sampling period of February 2012 was characterized by smoggy conditions; the daily limit of PM10 was consistently exceeded from 24 January until 21 February (Table 1). The average daily PM10 concentrations during January and February 2012 ranged from 15.9 to 281.3 μg/m^3 (automatic monitoring system, optoelectronic method, www.chmi.cz).

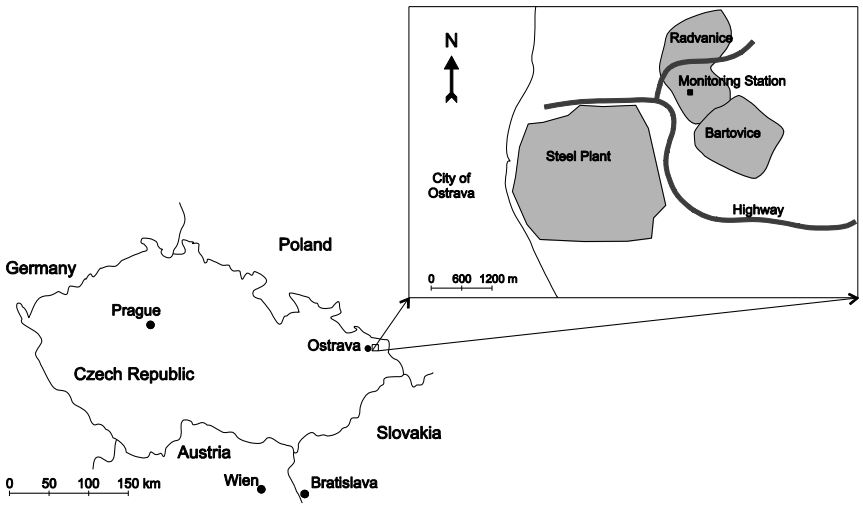

Fig. 1 Location of the study site. The detail shows positions of the steel plant and Radvanice and Bartovice suburban areas in relation to the monitoring station.

Table 1 List of particulate matter (PM) sample codes, corresponding sampling time and average daily concentration of PM10, and meteorological data. Note that values of concentration of PM10 were obtained using automatic optoelectronic method and represent 24-hour averages. Optoelctronic data for concentration of PM1 are not available.

Specimen Code		Sampling Period		PM10 [μg/m^3]	Air Pressure [hPa]	Humidity [%]	Temperature [°C]	Wind Speed [m/s]	Wind Direction
PM10	PM1	Start	End						
G180	G181	30/01/2012 09:00	30/01/2012 19:00	121.8	1031.0	65.7	-10.3	1.7	NE (ENE)
G178	G179	30/01/2012 19:00	31/01/2012 07:00		1030.8	78.3	-13.9	1.0	NE (ENE)
G176	G177	31/01/2012 07:00	31/01/2012 19:00	131.5	1029.4	71.6	-12.8	1.4	NE (ENE)
G174	G175	31/01/2012 19:00	01/02/2012 07:15		1028.4	75.7	-14.1	0.9	NE
G172	G173	01/02/2012 07:45	01/02/2012 19:00	103.5	1028.6	70.3	-14.2	2.2	NE
G170	G171	01/02/2012 19:00	02/02/2012 07:00		1028.9	76.8	-16.8	1.7	NE
G168	G169	02/02/2012 08:00	02/02/2012 19:00	228.7	1029.2	71.8	-15.6	1.4	N
G166	G167	02/02/2012 20:00	03/02/2012 07:00		1029.7	78.5	-17.7	0.9	NE (ENE)
G164	G165	03/02/2012 07:00	03/02/2012 19:00	180.6	1030.0	63.7	-16.0	1.8	NE (ENE)
G162	G163	03/02/2012 19:00	04/02/2012 07:00		1031.7	73.3	-18.2	1.3	NNE
G160	G161	04/02/2012 07:00	04/02/2012 19:00	147.4	1031.2	67.5	-16.4	1.7	NNE
G158	G159	04/02/2012 19:00	05/02/2012 07:00		1030.5	64.1	-15.0	1.5	NE (NNE)
G156	G157	05/02/2012 07:00	05/02/2012 19:00	127.1	1030.2	58.0	-13.2	2.1	NE (ENE)
G154	G155	05/02/2012 19:00	06/02/2012 07:00		1029.9	74.6	-15.5	1.2	NNE (ENE)
G152	G153	06/02/2012 07:00	06/02/2012 19:00	141.7	1028.8	72.8	-14.5	1.7	N (NNW, NNE)
G150	G151	06/02/2012 19:00	07/02/2012 07:00		1028.0	74.5	-13.6	2.2	NE (NNE)
G148	G149	16/02/2012 09:00	16/02/2012 19:00	49.5	1013.8	83.0	-2.9	1.8	NNW
G146	G147	16/02/2012 19:00	17/02/2012 07:00		1016.5	84.6	-3.1	1.4	W (NW, WSW)
G144	G145	17/02/2012 07:00	17/02/2012 19:00	62.8	1012.2	93.0	-1.3	1.9	SW (WWN)
G74	G143	17/02/2012 19:00	18/02/2012 07:00		1014.8	88.3	1.3	1.4	W (WSW, WNW)

Magnetic properties were measured using ADE EV9 vibrating sample magnetometer (DSM Magnetics, ADE Corporation; Lowell, MA, USA) at room temperature. Hysteresis loops (induced magnetization) were measured in magnetic fields from -2 to +2 T. In order to define the intersections with the field and magnetization axes using linear interpolation (coercive force B_c and saturation remanent magnetization M_{rs}, respectively), the field step varied from 0.5 mT to 50 mT for different sections of the loop, the finest field step was used around the intersection with the magnetization axis. From each sample, a specimen 1 cm wide and 10 cm long was cut, carefully folded and attached to the quartz sample holder using teflon tape. The measured magnetization represents a combination of different responses: that of diamagnetic substance of the filter and quartz sample holder, and diamagnetic, paramagnetic and ferrimagnetic minerals contained in the dust. In order to obtain only the signal corresponding to ferrimagnetic minerals (presumably magnetite), first background curve of the blank filter was subtracted from the measured data. Then, combined paramagnetic and diamagnetic linear contribution to magnetization of minerals present in the specimen was determined by linear regression fit above 1 T and subtracted from the whole hysteresis loop (Fig. 2). The measured data were normalized by mass of the measured dust m_{MD}, which was determined as follows:

$$m_{MD} \approx (m_{SP}/m_0)m_D,$$

where m_{SP} is mass of the measured specimen, m_0 is mass of the original sample (whole filter and deposited dust), and m_D is mass of the dust deposited on the whole filter. Distribution of the dust on the surface of the filter can be considered as sufficiently homogeneous (Sysalova et al., 2002).

Mass-normalized saturation induced magnetization M_s depends solely on the concentration of ferrimagnetic substance; in case of pure magnetite, M_s would be 90-92 Am^2/kg. Saturation remanent magentization M_{rs} depends on the concentration as well as on grain-size distribution of the ferrimagnetic substances. The ration M_{rs}/M_s reflects the squarness of the hysteresis loop and like coercive force B_c depends mostly on the grain-size distribution. Coarse, multidomain particles have

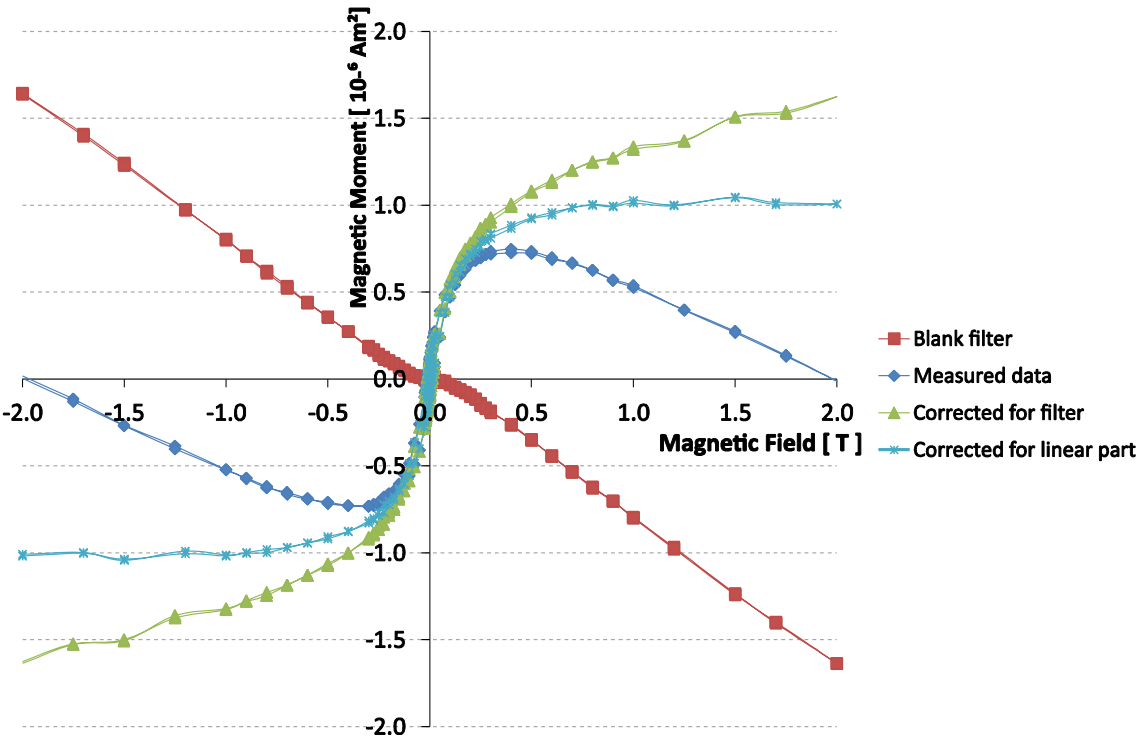

Fig. 2 Example of the measured hysteresis loop and data processing (correction for the background and linear diamagnetic and paramagnetic contributions).

low values of both M_{rs}/M_s and B_c, finer stable single-domain particles show higher values. Finally, ultra-fine, superparamagentic particles contribute neither to M_{rs} nor to B_c. For more details on these magnetic properties and their meaning, see, e.g., Dunlop and Ozdemir (1997).

Magnetic properties determined from the hysteresis loops (M_s, M_{rs} and B_c) were compared with the PM10 and PM1 concentrations of the corresponding samples collected by the high-volume samplers using bi-plots and linear regression.

Results and Discussion

Samples with the corresponding sampling period, concentration of PM10 obtained using automatic opetoelectronic method (about 12-hour averages, corresponding to the period of sampling by the high-volume samplers), and basic meteorological data are listed in Table 1. Table 2 shows the data of PM10 and PM1 concentrations determined from the dust collected by the high-volume samplers (about 12-hour sampling periods) and magnetic properties of the measured specimens (saturation

induced and remanent magnetizations and coercive force). It is obvious that except for one specimen (G148, day period towards the end of the sampling), the PM10 concentrations determined by the automatic monitoring system exceeded the allowed limit for daily average of 50 $\mu g/m^3$ (WHO, 2006). This is in good agreement with the PM10 concentrations determined from the collected samples of PM10, which were well above the limit of 50 $\mu g/m^3$ (except for three specimens at the end of the sampling period). Although the limit of 50 $\mu g/m^3$ represents the daily average and our data correspond to about 12-hours sampling period, we use this allowance limit for reference to emphasize that the sampling period was characterized by significantly increased levels of air pollution.

Saturation induced magnetization M_s of the PM10 specimens varies from 0.140 to 0.467 Am^2/kg. One specimen (G148) shows significantly increased value of 0.953 Am^2/kg. The average value of M_s is 0.351 Am^2/kg (including the G148 specimen). Three specimens (G146, G144 and G74) are considered as outliers, with M_s of 10.944, 14.971 and 14.733 Am^2/kg, respectively (Table 2). These three values are very high in terms of concentration of magnetite (100% magnetite would have M_s of 90-92 Am^2/kg, e.g., Dunlop and Ozdemir, 1997). The corresponding saturation remanent magnetization M_{rs} values are about 10 times lower, ranging from 0.014 to 0.051 Am^2/kg, specimen G148 has M_{rs} of 0.100 Am^2/kg. The average value of PM10 M_{rs} is 0.037 Am^2/kg. The three outliers (G146, G144 and G74) have Mrs of 0.998, 1.277 and 1.181 Am^2/kg, respectively (Table 2). Correlation of M_s and M_{rs} with the PM10 concentrations is shown in Fig. 3, where striking trend can be observed. Both parameters clearly show negative trend with the PM10 concentration, except for the three outliers (G146, G144 and G74), with the goodness of the fit R^2 of 0.449 and 0.473, respectively, suggesting moderately strong correlation.

Very similar observation was done in the case of PM1. M_s values vary from 0.066 to 0.293 Am^2/kg, with an average of 0.169 Am^2/kg. Again, three outliers were identified (G147, G145 and G143), coinciding in the sampling time with those of PM10. These have M_s of 8.448, 9.192 and 8.636

182 Am^2/kg, respectively. M_{rs} values are between 0.007 and 0.033 Am^2/kg, with an average of 0.018
183 Am^2/kg. The three outliers have M_{rs} of 0.779, 0.722 and 0.719 Am^2/kg, respectively (Table 2).
184 Correlation between M_{rs} and PM1 concentration is depicted in Fig. 4. Similar negative trend as in
185 Fig. 3 can be observed also in the case of PM1, with the R^2 parameter of 0.586 for M_s vs. PM1
186 (suggesting moderate correlation), and of 0.279 for M_{rs} vs. PM1, suggesting weak correlation.

187 Values of coercive force B_c are from 7.7 to 11.8 mT (average of 9.68 mT) for PM10, and between 4.8
188 and 12.3 mT (average of 7.81 mT) for PM1. Only week relationship between was observed, with R^2 of
189 0.1175 and 0.169, respectively (Fig. 5).

Table 2 List of magnetic parameters of the measured specimens and concentrations of the deposited PM10 and PM1. C_{oe}: concentration of PM obtained using automatic optoelectronic method (24-hour averages), C_{hv}: concentration of PM obtained using high-volume sampler samples (12-hour averages), M_s: saturation induced magnetization, M_{rs}: saturation remanent magnetization, B_c: coercive force.

PM10						PM1				
Code	**C_{oe} [$\mu g/m^3$]**	**C_{hv} [$\mu g/m^3$]**	**M_s [Am^2/kg]**	**M_{rs} [Am^2/kg]**	**B_c [mT]**	**Code**	**C_{hv} [$\mu g/m^3$]**	**M_s [Am^2/kg]**	**M_{rs} [Am^2/kg]**	**B_c [mT]**
G180	121.8	93.2	0.247	0.026	9.1	G181	52.6	0.140	0.012	7.8
G178		80.5	0.200	0.026	8.4	G179	39.7	0.152	0.018	7.4
G176	131.5	93.9	0.306	0.031	10.2	G177	49.5	0.170	0.022	9.1
G174		90.2	0.284	0.029	8.9	G175	45.7	0.163	0.017	6.5
G172	103.5	67.5	0.393	0.042	10.2	G173	30.7	0.172	0.015	12.3
G170		73.2	0.467	0.046	8.7	G171	39	0.293	0.033	7.5
G168	228.7	95.5	0.307	0.032	10.4	G169	73.6	0.104	0.010	8.3
G166		166.4	0.140	0.014	8.3	G167	103.8	0.066	0.010	5.3
G164	180.6	150.7	0.194	0.021	7.7	G165	59.8	0.113	0.012	4.8
G162		171.3	0.236	0.023	9.8	G163	70.5	0.127	0.020	8.2
G160	147.4	140.0	0.285	0.035	10.4	G161	56.6	0.175	0.018	6.8
G158		90.5	0.465	0.046	9.1	G159	40.8	0.225	0.021	9.0
G156	127.1	56.0	0.416	0.046	11.8	G157	25.9	0.243	0.031	7.8
G154		107.4	0.213	0.024	11.1	G155	49	0.098	0.014	8.4
G152	141.7	102.9	0.421	0.040	9.2	G153	46.3	0.146	0.007	7.8
G150		87.1	0.440	0.051	10.6	G151	32.8	0.244	0.026	7.4
G148	49.5	41.7	0.953	0.100	10.4	G149	27.5	0.249	0.017	5.8
G146		33.2	10.944	0.998	9.8	G147	17.9	8.448	0.779	8.5
G144	62.8	63.4	14.971	1.277	9.8	G145	29.4	9.192	0.722	8.0
G74		39.8	14.733	1.181	9.7	G143	17.9	8.636	0.719	9.4

While the saturation induced magnetization M_s values depend only on the concentration of ferrimagnetic fraction, the remanent magnetization M_{rs} is affected also by the grain-size distribution. Finer stable single-domain (SSD) particles have significantly higher values than coarse multi-domain (MD) particles. Ultra-fine nanosized superparamagnetic (SP) particles do not contribute to magnetic

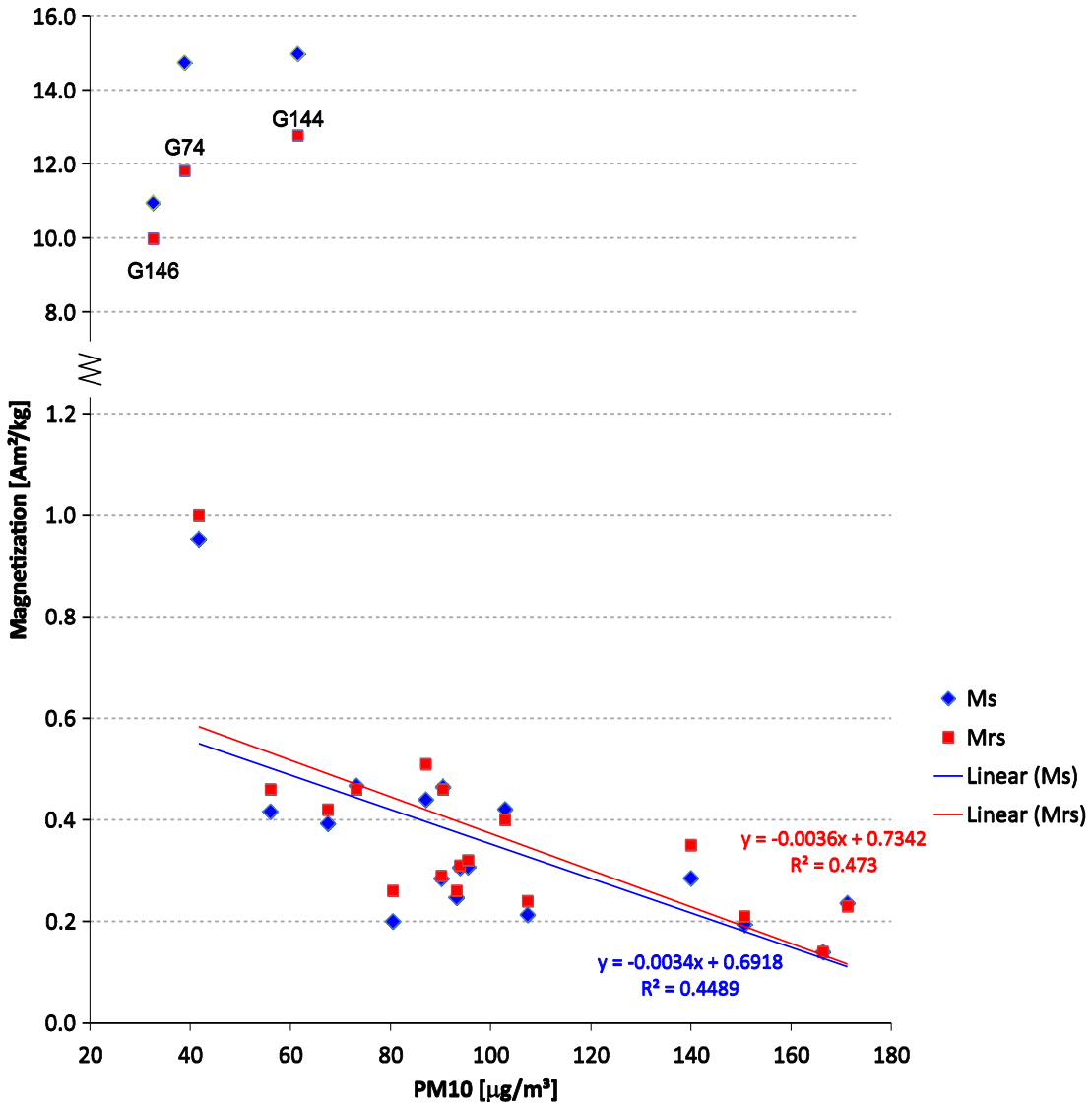

Fig. 3 Correlation between magnetization and concentration of PM10, collected by the high-volume sampler. M_s: saturation induced magnetization, M_{rs}: saturation remanent magnetization (values are multiplied by a factor of 10). Specimens G74, G144 and G146 are considered as outliers. R^2 is goodness of the fit parameter (coefficient of determination) of linear regression.

194 remanence. Theoretical value of M_{rs}/M_s for a system of non-interacting SSD particles is 0.5. In our
195 case, the values for PM10 specimens are from 0.080 to 0.129, with the average of 0.104. No outliers
196 were detected in this case and no correlation with PM10 concentration was observed. In case of PM1
197 specimens, M_{rs}/M_s ranges from 0.047 to 0.154, the average being 0.104. These values, along with the
198 very close similarity in relationship between M_s and M_{rs} on one side and PM concentration on the
199 other (Figs 3 and 4) clearly support the idea that the coarse MD particles dominate the collected PM
200 samples. However, both the M_s and M_{rs} values of PM10 are about twice of those of PM1 specimens,
201 suggesting that concentration of magnetite in PM10 is about two times higher than in PM1.

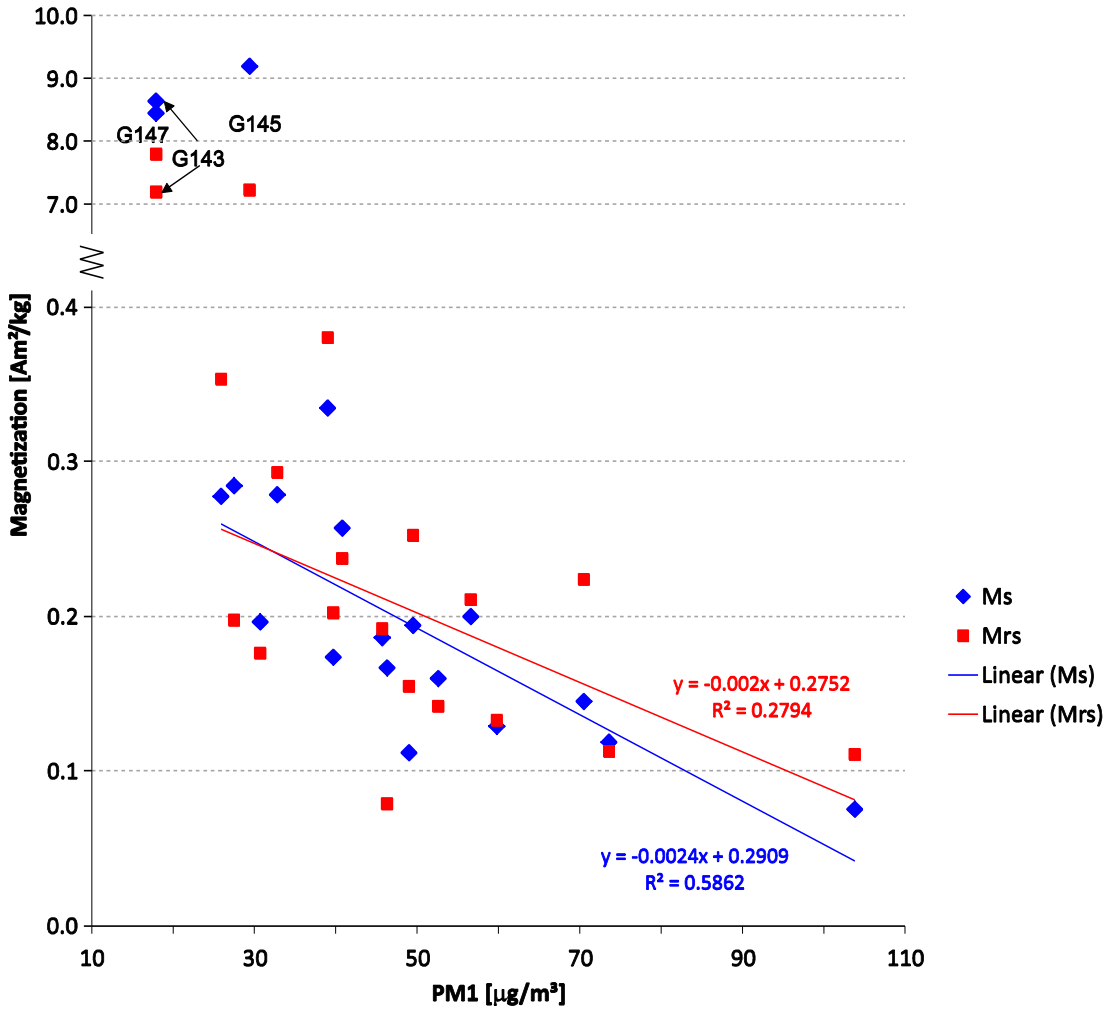

Fig. 4 The same as in Fig. 3, but for PM1. Here specimens G143, G145 and G147 are considered as outliers.

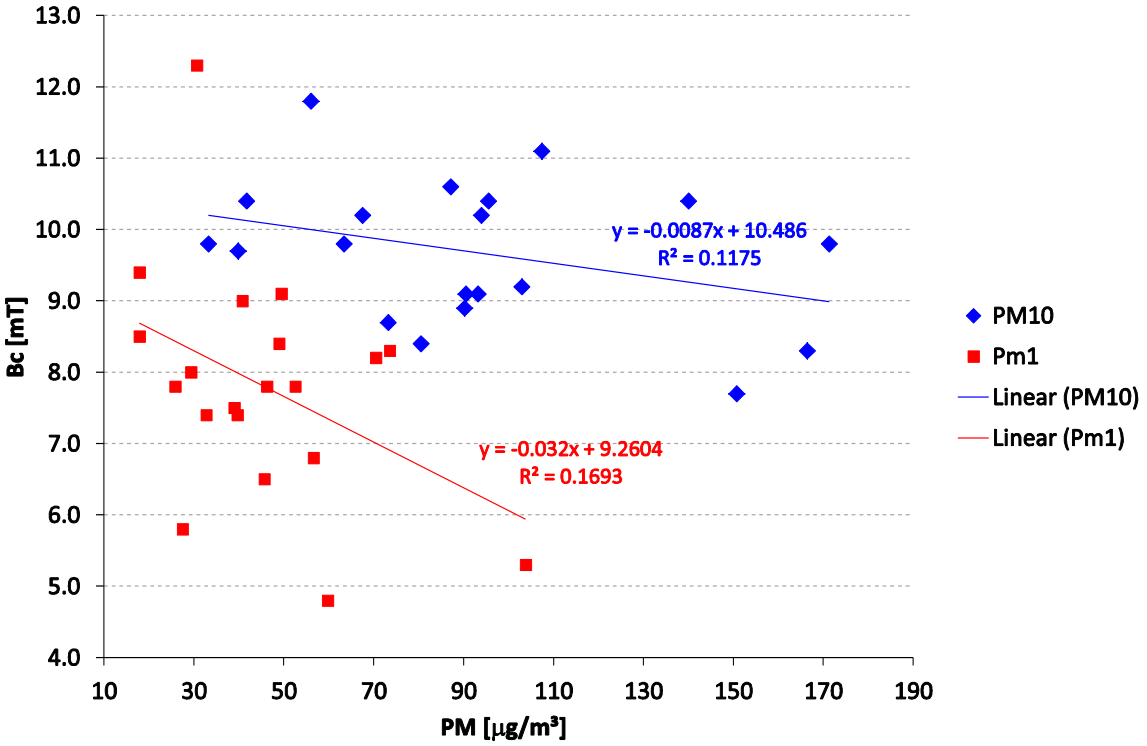

Fig. 5 Correlation between coercive force B_c and concentration of PM collected by the high-volume sampler.

Very similar relationship between concentration of ferrimagnetic iron oxides, expressed by M_s, and concentration of PM10 and PM1 suggest that composition of the particulate matter in both fractions is controlled by the same sources. However, the steel plant in the proximity does not contribute significantly to air pollution in these days. Somewhat weaker relationship between M_{rs} and PM1 may be explained by higher relative contribution of nano-sized SP magnetite particles, which do not contribute to magnetic remanence. However, situation is completely different during the days when the outliers where collected (at the end of the sampling smoggy period). These specimens show significantly higher values of M_s and M_{rs}, while the grain-size dependent B_c does not change. This can be interpreted as dominant contribution from the steel plant due to wind direction blowing from the plant to the monitoring station, while in the previous days it was blowing from the opposite direction.

213 It is interesting to see that the days with extremely high content of iron oxides (outliers in Figs 3
214 and 4) coincide not only with the change in the wind direction, but also with increased average daily
215 humidity and temperature, and decreased air pressure (Table 1). This may indicate worse
216 atmospheric circulation and dispersion of dust. However, elucidating this observation would require
217 much larger data set.

218 According to the information provided by the steel plant, special measures were in force during the
219 smoggy period. Namely, one baking belt with electrostatic filter in the southern part of the plant
220 stopped, while the remaining three belts with tissue filters in the northern side and one with
221 electrostatic filter in the southern side of the plant continued operation. This resulted in reduction of
222 production of this section by about 15%. Other specific actions were taken in different sections of the
223 plant with the aim to reduce dust emissions. These actions started on 28 January 2012 and lasted
224 until 16 February 2012. Thus, they fully covered our sampling period and we assume they did not
225 affect significantly our results, namely the pronounced change in the observed trend between
226 content of iron oxides and concentration of particulate matter.

227 **Conclusions**

228 Magnetic properties of day and night atmospheric dust samples of PM10 and PM1, collected by high-
229 volume samplers during smoggy period of winter 2012 at an industrial monitoring site located close
230 to major steel plant, were analyzed in comparison with the PM concentrations and local weather
231 conditions. Contrary to all the results published until now, our data show negative correlation
232 between the concentration of PM10 and saturation induced magnetization, which is a measure of
233 concentration of ferrimagnetic iron oxides magnetite and maghemite. The same results were
234 obtained also for PM1. Three distinct outliers, which do not follow this trend and show
235 magnetization values about 1.5 orders higher, were collected during days with the westerly's
236 prevailing wind (blowing from major city and steel plant) and changed weather conditions. We
237 believe that the iron-oxides content in the dust collected only during these days was controlled by

the emissions from the steel plant. During the other days, the complexity and high number of different pollution sources in the region, combined with the weather conditions (smoggy period) caused that the steel plant did not contribute significantly to air pollution at the nearby monitoring station. These are the first results showing such negative correlation between concentration of iron oxides and dust, which are striking in particular at site close to source of emissions rich in iron oxides. Despite that, our findings do not exclude magnetic methods from environmental monitoring. However, one has to realize that magnetic monitoring is site specific, reflects local conditions, and, as a first step, basic trendlines between the content of iron oxides and pollutants have to be determined at any new site.

List of Abbreviations

B_c	coercive force in T (magnetic field in direction opposite to previous saturation, at which induced magnetization changes its sign)
CHMI	Czech Hydrometeorological Institute
C_{hv}	concentration of PM determined from the mass of high-volume sampler samples before and after the sampling (12-hour averages)
C_{oe}	concentration of PM obtained using automatic optoelectronic method (24-hour averages)
m_0	mass of the original sample
m_{MD}	mass of the collected dust
M_{rs}	saturation remanent magnetization in Am^2/kg (magnetization in zero field after previous saturation)
M_s	saturation induced magnetization in Am^2/kg
m_{SP}	mass of the measured specimen
PM	particulate matter
PM1	particulate matter smaller than 1 micrometer
PM10	particulate matter smaller than 10 micrometers
R^2	goodness of the fit parameter (coefficient of determination) of linear regression

Declarations

Ethics approval and consent to participate:

Not applicable

Consent for publication:

Not applicable

Availability of data and material:

The datasets used and/or analysed during the current study are available from the corresponding author on reasonable request.

Competing interests:

The authors declare that they have no competing interests.

Funding:

The study was funded by the institutes of the authors, Czech Science Foundation project No. P210/10/0554, and Ministry of Education, Youth and Sports of the Czech Republic through an Inter-Vector project LVT19011.

Authors' contributions:

EP designed the study, and made substantial contribution to magnetic measurements, data interpretation and writing the manuscript. HG and AK made substantial contribution to magnetic measurements and data interpretation, and contributed to manuscript preparation. BK made substantial contribution to data interpretation, and contributed to manuscript preparation. HM collected the samples and provided meteorological data, and contributed to manuscript preparation.

Acknowledgements:

We are grateful for the support from the Czech Science Foundation Project No. P210/10/0554 and Ministry of Education, Youth and Sports of the Czech Republic through an Inter-Vector project LVT19011.

References

Brignole D, Drava G, Minganti V, Giordani P, Samson R, Vieira J, Pinho P, Branquinho C (2018) Chemical and magnetic analyses on tree bark as an effective tool for biomonitoring: A case study in Lisbon (Portugal). Chemosphere 195:508-514.

Chaparro MAE, Lavornia JM, Sinito AM (2013) Biomonitors of urban air pollution: Magnetic studies and SEM observations of corticolous foliose and microfoliose lichens and their suitability for magnetic monitoring Environ Pollut 172:61-69.

CHMI (2012) Znečištění ovzduší na území České republiky v roce 2012 (Air pollution over the territory of the Czech Republic in 2012). Annual Report. Czech Hydrometeorological Institute, Prague, http://portal.chmi.cz/files/portal/docs/uoco/isko/grafroc/groc/gr12cz/obsah.html (in Czech).

Dunlop DJ, Ozdemir O (1997) Rock Magnetism: Fundamentals and Frontiers. Cambridge University Press, Cambridge, U.K.

Fabian K, Reimann C, McEnroe SA, Willemoes-Wissing B (2011) Magnetic properties of terrestrial moss (Hylocomium splendens) along a north-south profile crossing the city of Oslo, Norway. Sci Tot Environ 409:2252-2260.

Hofman J, Maher BA, Muxworthy AR, Wuyts K, Castanheiro A, Samson R (2017) Biomagnetic Monitoring of Atmospheric Pollution: A Review of Magnetic Signatures from Biological Sensors. Environ Sci Technol 51:6648-6664.

Jordanova D, Petrov P, Hoffmann V, Gocht T, Panaiotu C, Tsacheva T, Jordanova N (2010) Magnetic signature of different vegetation species in polluted environment. Stud Geophys Geod 54:417-442.

Jordanova NV, Jordanova DV, Veneva L, Yorova K, Petrovsky E (2003) Magnetic response of soils and vegetation to heavy metal pollution - A case study. Environ Sci Technol 37:4417-4424.

Kardel F, Wuyts K, De Wael K, Samson R (2018) Biomonitoring of atmospheric particulate pollution via chemical composition and magnetic properties of roadside tree leaves. Environ Sci Pollut Res 25:25994-26004.

Kardel F, Wuyts K, Maher BA, Hansard R, Samson R (2011) Leaf saturation isothermal remanent magnetization (SIRM) as a proxy for particulate matter monitoring: Inter-species differences and in-season variation. Atmos Environ 45:5164-5171.

Kardel F, Wuyts K, Maher BA, Samson R (2012) Intra-urban spatial variation of magnetic particles: Monitoring via leaf saturation isothermal remanent magnetisation (SIRM). Atmos Environ 55:111-120.

Kodnik D, Winkler A, Carniel FC, Tretiach M (2017) Biomagnetic monitoring and element content of lichen transplants in a mixed land use area of NE Italy. Sci Tot Environ 595:858-867.

Lehndorff E, Urbat M, Schwark L (2006) Accumulation histories of magnetic particles on pine needles as function of air quality. Atmos Environ 40:7082-7096.

Limo J, Paturi P, Makinen J (2018) Magnetic biomonitoring with moss bags to assess stop-and-go traffic induced particulate matter and heavy metal concentrations. Atmos Environ 195:187-195.

Maher BA, Moore C, Matzka J (2008) Spatial variation in vehicle-derived metal pollution identified by magnetic and elemental analysis of roadside tree leaves. Atmos Environ 42:364-373.

Marie DC, Chaparro MAE, Irurzun MA, Lavornia JM, Marinelli C, Cepeda R, Bohnel HN, Miranda AGC, Sinito AM (2016) Magnetic mapping of air pollution in Tandil city (Argentina) using the lichen Parmotrema pilosum as biomonitor. Atmos Pollut Res 7:513-520.

Marie DC, Chaparro MAE, Lavornia JM, Sinito AM, Miranda AGC, Gargiulo JD, Bohnel HN (2018) Atmospheric pollution assessed by in situ measurement of magnetic susceptibility on lichens. Ecol Indic 95:831-840.

Matzka J, Maher BA (1999) Magnetic biomonitoring of roadside tree leaves: identification of spatial and temporal variations in vehicle-derived particulates. Atmos Environ 33:4565-4569.

Mitchell R, Maher BA (2009) Evaluation and application of biomagnetic monitoring of traffic-derived particulate pollution. Atmos Environ 43:2095-2103.

Mitchell R, Maher BA, Kinnersley R (2010) Rates of particulate pollution deposition onto leaf surfaces: Temporal and inter-species magnetic analyses. Environ Pollut 158:1472-1478.

Moreno E, Sagnotti L, Dinares-Turell J, Winkler A, Cascella A (2003) Biomonitoring of traffic air pollution in Rome using magnetic properties of tree leaves. Atmos Environ 37:2967-2977.

Muxworthy AR, Matzka J, Petersen N (2001) Comparison of magnetic parameters of urban atmospheric particulate matter with pollution and meteorological data. Atmos Environ 35:4379-4386.

Muxworthy AR, Matzka M, Davila AF, Petersen N (2003) Magnetic signature of daily sampled urban atmospheric particles. Atmos Environ 37:4163-4169.

Paoli L, Winkler A, Guttova A, Sagnotti L, Grassi A, Lackovicova A, Senko D, Loppi S (2017) Magnetic properties and element concentrations in lichens exposed to airborne pollutants released during cement production. Environ Sci Pollut Res 24:12063-12080.

Petrovsky E, Zboril R, Grygar TM, Kotlik B, Novak J, Kapicka A, Grison H (2013) Magnetic particles in atmospheric particulate matter collected at sites with different level of air pollution. Stud Geophys Geod 57:755-770.

Rachwal M, Rybak J, Rogula-Kozlowska W (2018) Magnetic susceptibility of spider webs as a proxy of airborne metal pollution. Environ Pollut 234:543-551.

Rodriguez-Germade I, Mohamed KJ, Rey D, Rubio B, Garcia A (2014) The influence of weather and climate on the reliability of magnetic properties of tree leaves as proxies for air pollution monitoring. Sci Tot Environ 468:892-902.

Sagnotti L, Macri P, Egli R, Mondino M (2006) Magnetic properties of atmospheric particulate matter from automatic air sampler stations in Latium (Italy): Toward a definition of magnetic fingerprints for natural and anthropogenic PM10 sources. J Geophys Res-Solid Earth DOI: 10.1029/2006JB004508.

Sagnotti L, Taddeucci J, Winkler A, Cavallo A (2009) Compositional, morphological, and hysteresis characterization of magnetic airborne particulate matter in Rome, Italy. Geochem Geophys Geosyst DOI: 10.1029/2009GC002563.

Salo H, Berisha AK, Makinen J (2016a) Seasonal comparison of moss bag technique against vertical snow samples for monitoring atmospheric pollution. J Environ Sci 41:128-137.

Salo H, Bucko MS, Vaahtovuo E, Limo J, Makinen J, Pesonen LJ (2012) Biomonitoring of air pollution in SW Finland by magnetic and chemical measurements of moss bags and lichens. J Geochem Explor 115:69-81.

Salo H, Makinen J (2014) Magnetic biomonitoring by moss bags for industry-derived air pollution in SW Finland. Atmos Environ 97:19-27.

370 Salo H, Makinen J (2019) Comparison of traditional moss bags and synthetic fabric bags in magnetic
371 monitoring of urban air pollution. Ecol Indic 104:559-566.

372 Salo H, Paturi P, Makinen J (2016b) Moss bag (Sphagnum papillosum) magnetic and elemental
373 properties for characterising seasonal and spatial variation in urban pollution. Int J Environ Sci
374 Technol 13:1515-1524.

375 Sysalova J, Kucera J, Kotlik B, Havranek V (2002) Quality control materials for the determination of
376 trace elements in airborne particulate matter. Anal Bioanal Chem 373:195-199.

377 Urbat M, Lehndorff E, Schwark L (2004) Biomonitoring of air quality in the Cologne conurbation using
378 pine needles as a passive sampler - Part I: magnetic properties. Atmos Environ 38:3781-3792.

379 Vezzola LC, Muttoni G, Merlini M, Rotiroti N, Pagliardini L, Hirt AM, Pelfini M (2017) Investigating
380 distribution patterns of airborne magnetic grains trapped in tree barks in Milan, Italy: insights for
381 pollution mitigation strategies. Geophys J Int 210:989-1000.

382 Vukovic G, Urosevic MA, Goryainova Z, Pergal M, Skrivanj S, Samson R, Popovic A (2015a). Active
383 moss biomonitoring for extensive screening of urban air pollution: Magnetic and chemical analyses.
384 Sci Tot Environ 521:200-210.

385 Vukovic G, Urosevic MA, Tomasevic M, Samson R, Popovic A (2015b) Biomagnetic monitoring of
386 urban air pollution using moss bags (Sphagnum girgensohnii). Ecol Indic 52:40-47.

387 WHO (2006) WHO Air quality guidelinesfor particulate matter,ozone, nitrogendioxide and sulfur
388 dioxide. World Health Organization, Geneva, Switzerland.

389 Wuyts K, Hofman J, Van Wittenberghe S, Nuyts G, De Wael K, Samson R (2018) A new opportunity for
390 biomagnetic monitoring of particulate pollution in an urban environment using tree branches. Atmos
391 Environ 190:177-187.

392 Zhang CX, Huang BC, Li ZY, Liu H (2006) Magnetic properties of high-road-side pine tree leaves in
393 Beijing and their environmental significance. Chinese Sci Bull 51:3041-3052.

394 Zhang CX, Huang BC, Liu QS (2009) Magnetic properties of different pollution receptors around steel
395 plants and their environmental significance. Chinese J Geophys-Chinese Edition 52:2826-2839.

396 Zhang CX, Huang BC, Piper JDA, Luo RS (2008) Biomonitoring of atmospheric particulate matter using
397 magnetic properties of Salix matsudana tree ring cores. Sci Tot Environ 393:177-190.

398